Deep Space Optical Communications (DSOC) Downlink Simulation with Varying PPM Order

Emmanuel Domfeh Aboagye (eadomfeh@yahoo.com)
Darmstadt University of Applied Sciences https://orcid.org/0000-0003-2888-3565
Shun-Ping Chen
Darmstadt University of Applied Sciences

Original Research

Keywords: Deep Space Optical Communications (DSOC), Pulse Position Modulation (PPM), Photon Counting, Intensity Modulation, Photon Efficiency, Channel Capacity

Posted Date: February 11th, 2021

DOI: https://doi.org/10.21203/rs.3.rs-185923/v1

Deep Space Optical Communications (DSOC) Downlink Simulation with Varying PPM Order

Emmanuel Domfeh Aboagye, Shun-Ping Chen

Emmanuel Domfeh Aboagye, Ing., MBA, MSc.

Institute of Communication Technologies, Darmstadt University of Applied Sciences, Birkenweg 8, D-64295 Darmstadt, Germany

+491785265985 or +4915216863621

emmanuel.d.aboagye@stud.h-da.de or eadomfeh@yahoo.com

Shun-Ping Chen, Prof. Dr.

Institute of Communication Technologies, Darmstadt University of Applied Sciences, Birkenweg 8, D-64295 Darmstadt, Germany

+496151.1638258

shun-ping.chen@h-da.de

ABSTRACT: During the course of a typical deep space mission like Mars Earth mission, there exist a wide range of operating points due to the different changes in geometry that consequently cause different Link Budgets in terms of received signal and noise power. These changes include: Distance Range, Sun-Earth-Planet Angle, Zenith Angle and Atmospheric conditions. The different operating points with different losses (background noise, pointing losses and atmospheric losses) lead to different capacities and data rates over the course of a typical Deep Space mission. Consequently, different engineering parameters are adjusted and optimized to combat some of these varying losses in order to get an acceptable data rate and bit error probabilities. This provides a good basis to undertake analysis and simulations of the various operating conditions that occur with the varying spatial orbital time periods on the resulting received signal power level, noise power level, capacity, data rates and bit error probabilities. This paper details results of simulations done in a typical Deep Space Optical Communication link operation.

KEYWORDS: Deep Space Optical Communications (DSOC); Pulse Position Modulation (PPM); Photon Counting; Intensity Modulation; Photon Efficiency; Channel Capacity

DECLARATIONS

We declare that this manuscript presented is our own work.
Areas or formulas used in the simulation that were quoted from other sources have their references provided.

Funding

Not Applicable

Conflicts of interest/Competing interests

Not Applicable

Availability of data and material (data transparency)

We declare that the data and material that were generated from our own work in the simulation results were used in this manuscript.

Code availability (software application or custom code)

We declare that the code that was used to generate the simulations in this manuscript are the results of our own work and are available.

Authors' contributions

This manuscript simulates the impact of varying the pulse position modulation (PPM) order for a deep space optical communication system in order to optimize the data rates and bit error probabilities in varying operating points and conditions. It helps to understand reasons why PPM orders of 64/128/256 are optimum values among the range of 2-4096 in order to achieve high data rates.

Abbreviations

PPM : Pulse Position Modulation; APD : Avalanche Photo Detector; M-nary : PPM Order; AU : Astronomical Units; BEP : Bit Error Probability; SEP : Symbol Error Probability; BER : Bit Error Rate; Tx : Transmitter; Rx : Receiver; DSOC: Deep Space Optical Communications

1 INTRODUCTION

There has been a paradigm shift in the use of radio communication to optical communication in the field of deep space optical communication during the last decade. The reason for this increasing interest for the applications of optical communications in deep space is due to its unique attributes such as large bandwidth, license free spectrum, high data rate, efficient power utilization and low mass requirements.

Deep space communications (DSOC) involves a distant communication link that focuses mainly on the transmission between the planetary objects that are hundred thousands or millions of kilometers apart. One famous example is the communication link between the earth and a spacecraft surrounding another planet such as Mars. The distance range between these planetary objects is granulated in astronomical units (AU).

This paper details results of simulations conducted in a typical Deep Space Optical Communication Mars-Earth link operation. During the course of a typical Mars-Earth mission, there exist a wide range of operating points due to the different changes in geometry that consequently leads to different Mars-Earth link budgets in terms of received signal and noise power. Examples of these changes during the course of the Mars-Earth mission include: distance range, sun-earth-planet angle, zenith angle and atmospheric conditions.

These different operating points can cause different losses (background noise, pointing losses and atmospheric losses) leading to different capacities and data rates over the course of a typical Mars Earth mission. Consequently, different parameters are adjusted to combat some of these varying losses in order to get an acceptable data rate and bit error probabilities. Thus, over the course of the typical

Mars-Earth mission, there will be varying noise power levels and received signal power levels due to the varying orbital time periods. For example, there will be orbital time instances when the Sun will come between mars and earth leading to higher level of noise and also higher distance range between the mars and the earth (the largest distance between earth and mars is about 225 million km) [2]. Conversely, in other orbital time instances, there will be situations where the Sun will not come in between mars and earth. This causes lower level of noise and also lower distance range between the Mars and the Earth (thus the earth is closest to mars 56 million km) [2]. The difference in the ranges of these two distinct positions over an orbital period (2.2 years) is approximately by a factor of 4. These lead to different capacities, data rates and bit error probabilities in these different conditions. Different engineering input parameters are adjusted accordingly to maintain or improve the data rates and bit error rates as the spatial orbital time period varies.

This provides a good basis to undertake analysis and simulations of the various operating conditions that occur with the varying spatial orbital time periods on the resulting received signal power level, noise power level, capacity, data rates and bit error probabilities.

In the subsequent pages of this paper, deep space optical communication system is modeled and simulated by using Matlab. The impact of optimization of received signal photons, noise photons, channel capacity, data rates and bit error rates through tuning and adjustment of the various parameters such as PPM order, laser transmitter aperture size, receiver aperture size and laser transmit power is also analyzed in this paper. Photon counting model in a non-coherent detection system setup for intensity modulation was used in these simulations to determine the photon counts at the receiver side and consequently recover the data transmitted. This is because non-coherent detection is the best for energy efficiency which is indispensable in space. Furthermore, Pulse-Position-Modulation (PPM) was used in the downlink simulations due to higher energy efficiency with low duty cycles compared with On-Off-Keying (OFF) in deep space when transmitting from Mars to Earth. [6]

2 DSOC SYSTEMS

2.1 DSOC MODEL BLOCK DIAGRAM

The deep space optical communication DSOC system model consists of the laser transmitter Tx, Tx aperture gain, DSOC Channel, Rx aperture gain and the APD receiver Rx. Figure 1 below shows a block diagram of the model.

Fig.1 Block diagram of a DSOC model.

2.2 DSOC MODEL EQUATIONS

In M-PPM, each symbol interval is divided into M time slots and a non-zero optical pulse is placed in one of these time slots while other slots are kept vacant. Moreover, for the purpose of synchronization additional slots called synchronization slots are added. For long distance or deep space communications, M-PPM scheme is widely used because it provides a high peak-to-average power ratio (PAPR) that improves its average-power efficiency [7]. Since k number of bits are sent per symbol, the average number of signal counts required per bit is divided by k, which makes it more energy efficient than OOK modulation for k > 2. Furthermore, unlike OOK, M-PPM does not require an adaptive threshold. However, M-PPM scheme has poor bandwidth efficiency at higher values of M. Downlink simulations were done for PPM order ranging from 2 to 4096; nevertheless 4 to 256 is typically used in the deep space mission for Mars [1].

The average power for M-PPM can be calculated as:

$$P_{avg} = \frac{(P_{max} + P_{min}\,(M-1))}{M} \qquad \leftarrow 1 \leftarrow$$

The time width of signal slot *Ts* is given by the equation depending on the parameter *Br*:

$$Ts = \frac{1}{PRR} \qquad \leftarrow 2 \leftarrow$$

The pulse repetition rate *PRR* required for a system with PPM order M, bit rate BR and bits k is given by the equation as:

$$PRR = \frac{M\ BR}{k} \qquad (3)$$

The free space loss *FSL* is given by the equation:

$$FSL = 20 \log\left(\frac{4\pi d}{\lambda}\right) \qquad (4)$$

The background radiation interferes with the received signal with the received signal. Object producing light such as the sun, the stars and earthshine may interfere with the received signal and cause background noise. Received background power P_b depends in the background irradiance, effective receive area, receiver field of view, optical filter bandwidth and the optical efficiency.

$$P_b = H_b\, A_{rec}\, \gamma_{fou}\, \Delta\lambda_{nr} \qquad (5)$$

where H_b is the background irradiation energy density (W/m^2/sr/µm), A_{rec} is the effective receive area (m^2), γ_{fou} is the receiver field of view measured in steradians (sr), $\Delta\lambda_{nr}$ is the optical filter bandwidth (µm) and nr is the optical efficiency of the receiver (scalar). The receiver field of view is given by

$$\gamma_{fou} = \frac{\pi}{4}\, \theta^2{}_{fou} \qquad (6)$$

Where θ_{fou}represent the planar angular detector field of view (radians) and depends on the telescope aperture. The value of Sky radiance, H_b ranges 0.007-0.015 W/(cm^{2}srµm) depending on the zenith angle and the time of daylight. [1]

Incident light at the APD is converted into electrical signals proportional to the power and the responsivity which is given by:

$$R = \frac{q\, n}{h\, f} \qquad (7)$$

Where, q is the electron charge, n the quantum efficiency, h Planck's constant and f is the optical frequency.

In order to build a realistic APD receiver, noises originated by the diode were considered. Shot noise depends on the average current from different sources was modeled by the equation:

$$\sigma^2{}_{sn} = 2\, q\, R\, Pr\, G^2\, F\, Bw \qquad (8)$$

Where G is the optical amplifier gain, P_r is the incident received optical power, B_w is the electrical bandwidth.

F is the excess noise factor of the APD and is given by:

$$F = k_{eff}\,G + (1 - k_{eff})\left(2 - \frac{1}{G}\right) \quad \leftarrow 9 \leftarrow$$

Where k_{eff} is the ratio of the hole and electron ionization coefficients.

Background shot noise is produced by the same process as signal shot noise and is given by

$$\sigma^2{}_{bg} = 2\,q\,R\,P_b\,G^2\,F\,B_w \quad \leftarrow 10 \leftarrow$$

Where P_b represents the background power.

The dark current shot noise is given by:

$$\sigma^2{}_{dc} = 2\,q\,F\,G^2\,I_b\,B_w + 2\,q\,I_s\,B_w \quad \leftarrow 11 \leftarrow$$

Where I_b is bulk leakage current which becomes amplified and I_s the surface leakage current which does not pass through the avalanche region.

The thermal noise is given by

$$\sigma^2{}_{th} = \frac{4\,k_B\,Tr\,F\,Bw}{RL} \quad \leftarrow 12 \leftarrow$$

Where R_L is the load resistance, T_r the electronic system noise temperature, and k_B the Boltzmann constant. The temperature T_r is the equivalent temperature of the loss and is usually the physical temperature of the load resistor.

Aggregating all currents and noise current sources, the mean and variance of the total output from the receiver can be derived. Two scenarios are considered: when a signal pulse is received and the time between when there is no pulse received. The mean output current from the receiver when a pulse is present is given by:

$$\mu_1 = R\,G\,P_{r1} + R\,G\,P_b + G\,I_b + I_s \quad \leftarrow 13 \leftarrow$$

$$\mu_0 = R\,G\,P_{r0} + R\,G\,P_b + G\,I_b + I_s \quad \leftarrow 14 \leftarrow$$

Where the index "1" denotes a received pulse and a "0" denotes the absence of a pulse. The variance of the output current is given by

$$\sigma^2{}_1 = \sigma^2{}_{sn1} + \sigma^2{}_{bg} + \sigma^2{}_{dc} + \sigma^2{}_{th} \quad \leftarrow 15 \leftarrow$$

$$\sigma^2{}_0 = \sigma^2{}_{sn0} + \sigma^2{}_{bg} + \sigma^2{}_{dc} + \sigma^2{}_{th} \quad \leftarrow 16 \leftarrow$$

The capacity of the DSOC was determined from equation

$$C = (log_2 e)\frac{\lambda}{M}\left[\left(1 + \frac{1}{\rho}\right)(In(1+\rho)) - \left(1 + \frac{M}{\rho}\right)In\left(1 + \frac{\rho}{M}\right)\right] \quad \leftarrow 17 \leftarrow$$

$\rho = \frac{\lambda S}{\lambda B}$ is the (detected) peak received signal power to background power. [1]

The signal to noise ratio (SNR) is determined and the bit error rate is calculated from these variance and mean output currents [4, 5]. Simulations of the received signal photons, noise photons, channel capacity and data rate are also computed accordingly [1, 8]. All equations were obtained from reference [1]. Table 1 gives

the list of parameters and values used for the simulation [3]. Synchronization slots were not considered in the simulations.

TABLE 1 PARAMETERS FOR SIMULATIONS

NAME	SYMBOL	VALUE	UNIT
Planck's Constant	H	6.624 × 10−34	Joules/Hertz
Electron charge	Q	1.6 × 10-19	Coulombs
Boltzmann's constant	K_b	1.38 × 10−23	Joules/Kelvin
Load resistance	R_L	5.75 × 1012 × Ts	Ohms
Elevation	Θ	20	Degrees
Signal slot width	T_s	Variable	Seconds
Laser Tx Power	P_{tx_avg}	5.0	Watt
Tx Aperture Diameter	D_{tx}	0.22	Meters
Rx Aperture Diameter	D_{rx}	5.0	Meters
Link Margin	L_{margin}	3.0	dB
Detector Efficiency	$\eta_{Detector}$	0.35	
Pointing Loss	L_{Point}	2	dB
Transmission Loss	L_{Trans}	0.55	
Wavelength	Λ	1.55	µm
Code Rate	R_{code}	0.45	
PPM Order	M	Variable	
Bits per Symbol	K	Variable	Bits
Pulse Repetition Rate	PRR	Variable	Pulses/second
Sky Radiance	H_b	0.0085	W/(cm^2 sr µm)
Bit Rate	BR	100	Mbit/s

3 SIMULATIONS OF VARYING PPM ORDER (M)

Simulations were done to investigate the impact of varying PPM order (M = 2, 4, 8, 32, 64, 128, 256, 512, 1024, 2048 and 4096) on the received signal photons, noise photons, channel capacity, bit error probability, bit error rate and data rates in relation to the distance range dependence. All other parameters remained unchanged for the simulation. The figures below show the results of the simulations.

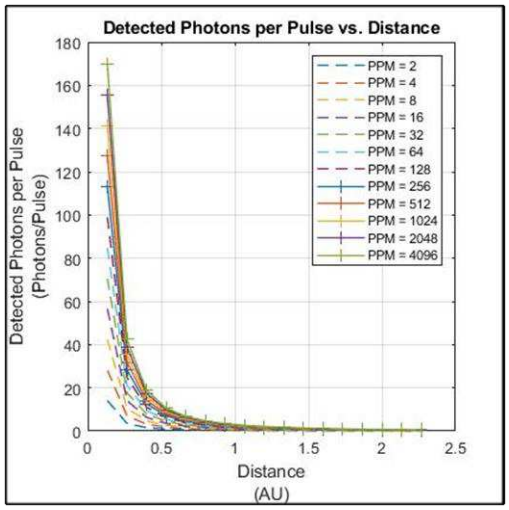

Figure 3.1

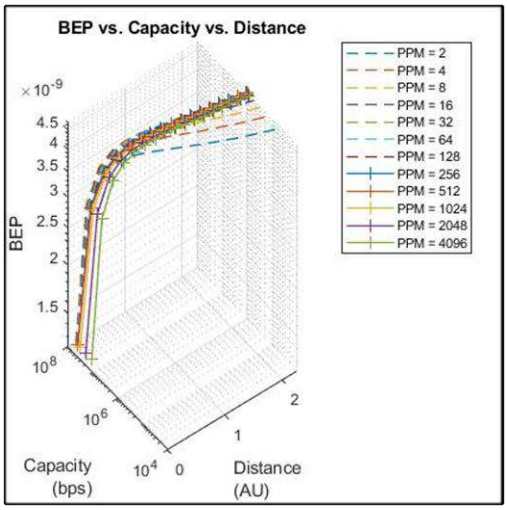

Figure 3.2

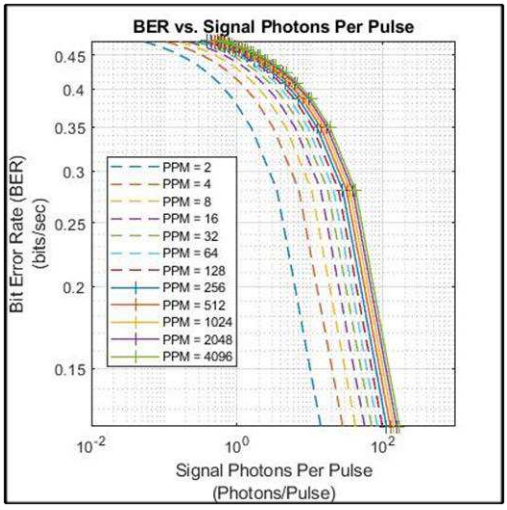

Figure 3.3

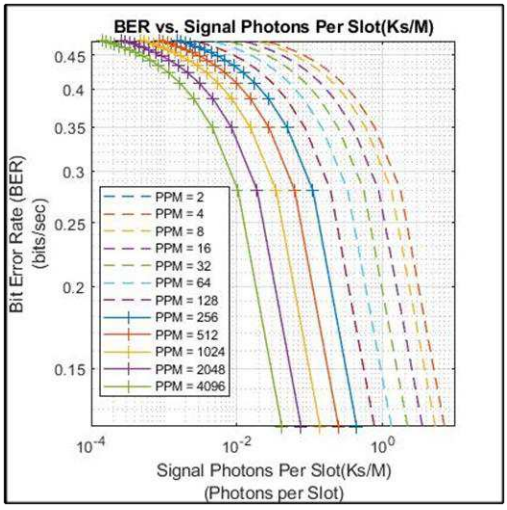

Figure 3.4

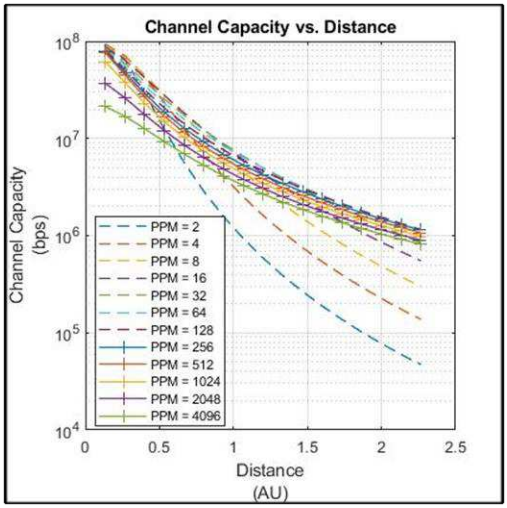

Figure 3.5

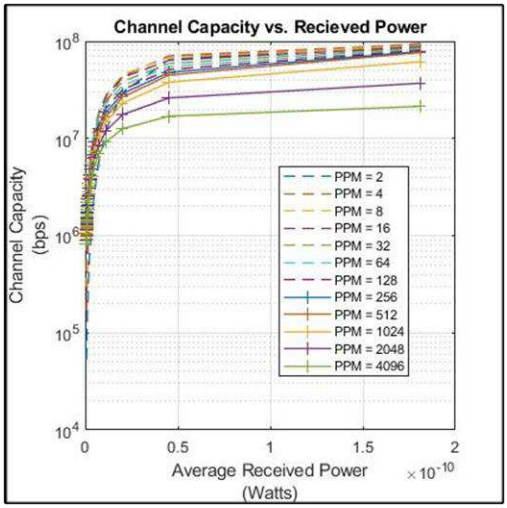

Figure 3.6

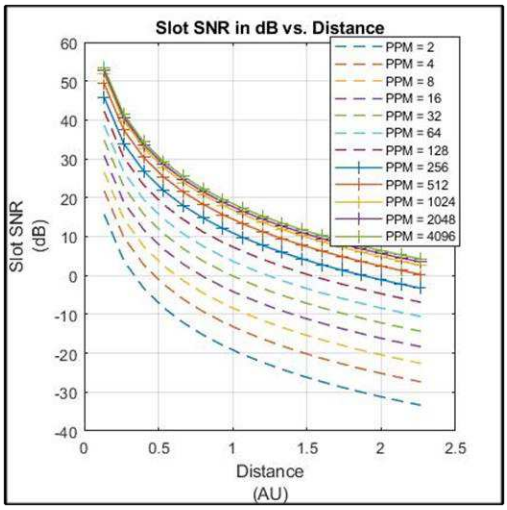

Figure 3.7

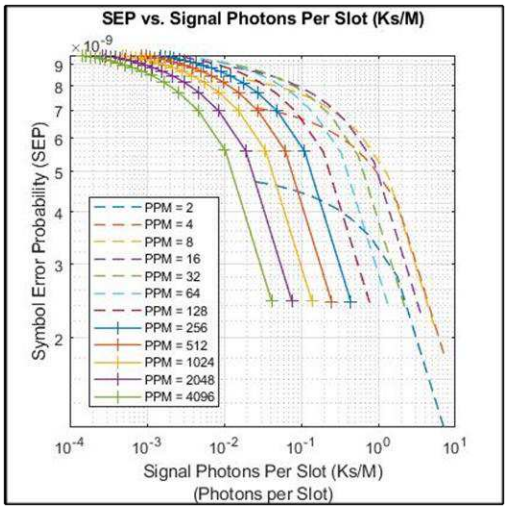

Figure 3.8

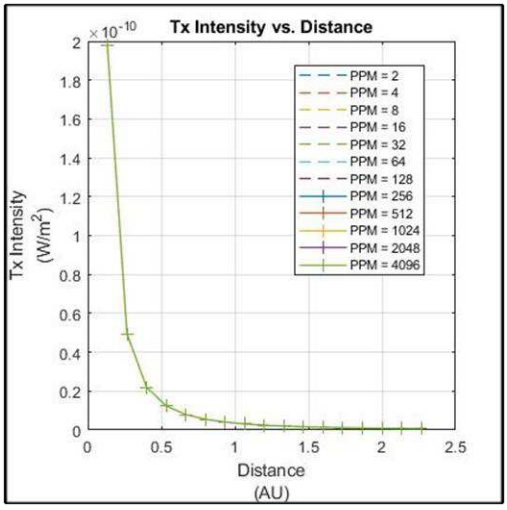

Figure 3.9

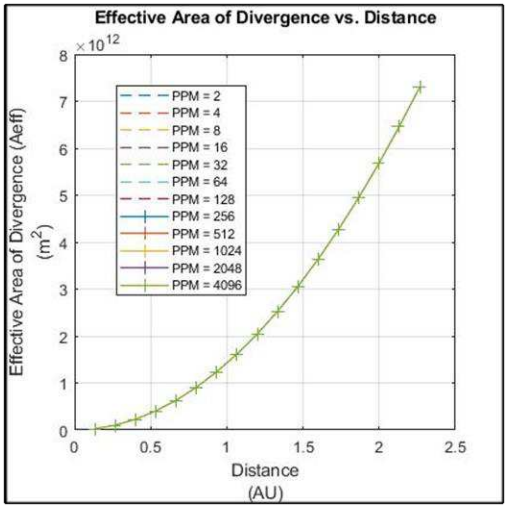

Figure 3.10

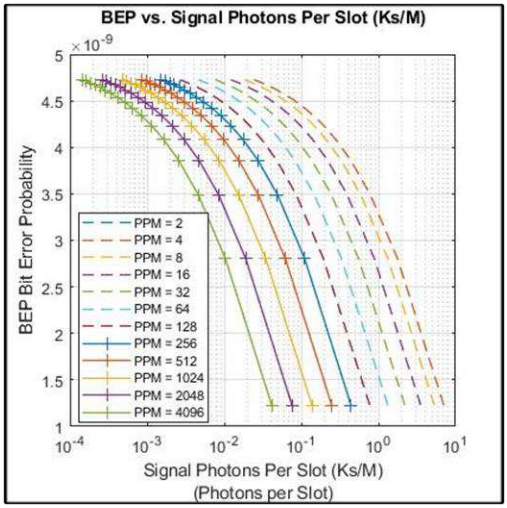

Figure 3.11

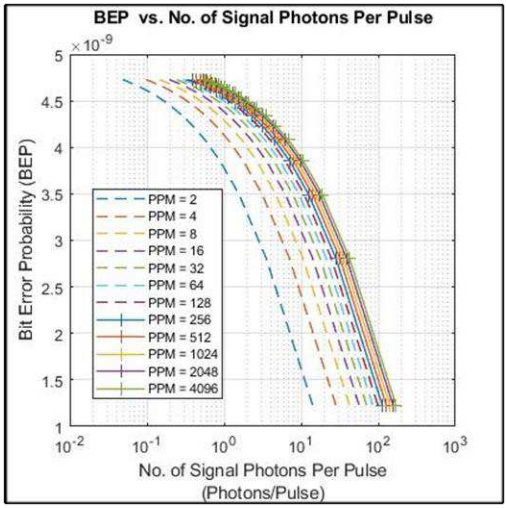

Figure 3.12

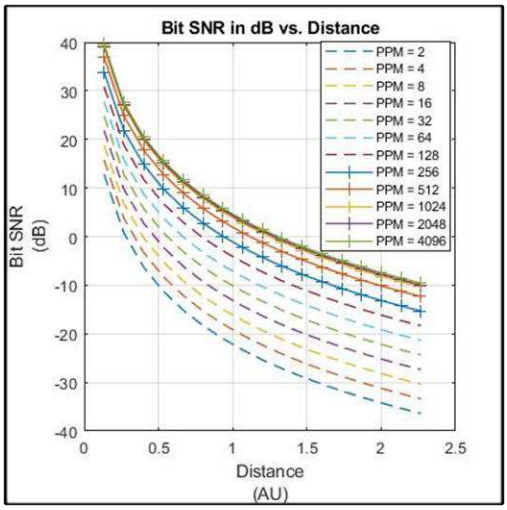

Figure 3.13

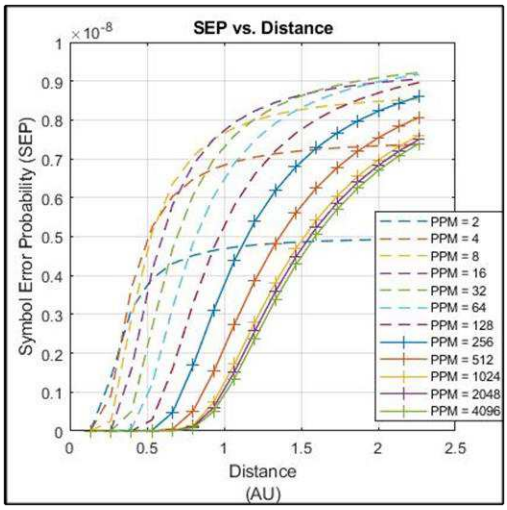

Figure 3.14

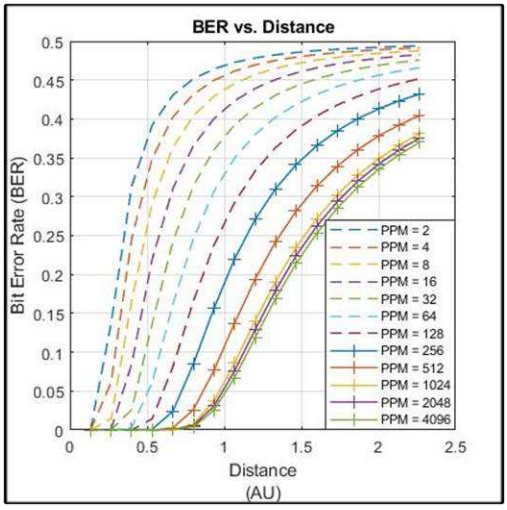

Figure 3.15

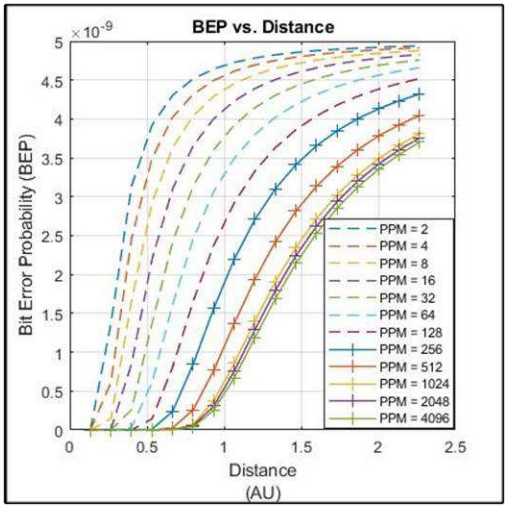

Figure 3.16

4 ANALYSIS OF VARYING PPM ORDER (M)

Figure 3.1shows that the detected signal photons decrease with increasing distance for a particular constant PPM order. Concurrently, the figure also depicts that for a specific constant distance range, higher PPM orders give rise to higher photon counts.

Figures 3.1, 3.2, 3.7 and 3.13 indicate that for a given constant PPM order, the channel capacity/data rate, slot SNR and bit SNR of the DSOC system decreases with increasing distance. Concurrently, for a specific constant distance range, very high PPM orders give rise to lower channel capacity and data rates.

Figures 3.9 and 3.10 show that the transmitter intensity and the effective area of divergence are unaffected by variation in the PPM order. Concurrently, it can be seen that the transmitter intensity of the laser reduces with increasing distance whereas the effective area of divergence increases with increasing distance.

Figures 3.3, 3.4, 3.8, 3.11 and 3.12 indicate that BER, BEP and SEP reduce with increasing number of detected signal photons. Concurrently, these figures show that the BER, BEP and SEP increase with increasing distance range of DSOC channel. Moreover, for a specific constant distance range, higher PPM orders give rise to lower BEP, BER and SEP.

Figures 3.2 gives a 3D pictorial view of how the Channel Capacity and BEP vary with distance range for different values of PPM order. It also shows that for a constant PPM order, the photons/pulse and the photons/bit decreases with increasing distance. Furthermore, for a specific constant distance range, higher PPM orders give rise to lower number of photon counts per bit.

Figures 3.5, 3.7 and 3.13 show that for a specific distance, improvement in Channel Capacity, Bit SNR and Slot SNR reaches a form of saturation when the PPM order is even increased above 128. This is the reason why PPM Order 128 is the most practically used modulation in Earth-Mars missions.

5 CONCLUSION

Simulation results have confirmed that optimization to improve the receive signal power (or received signal photons) can be accomplished by varying the PPM order. This can help to improve the ratio of the received signal photons to noise photon ratio. Thus, increasing M can improve the capacity, bit error probability, bit error rate and achievable data rate of the DSOC system. Nevertheless, that leads to less bandwidth efficiency. In addition to the effective delivery of the signal to the detector, the performance of the optical link also depends on the receiver sensitivity (measured in terms of received photons per bit). Because of the high cost associated with increasing the transmit power and system aperture, improving the receiver sensitivity is an important factor in the deep space optical communication system design. Thus optimizing the value of the PPM Order (by choosing high M) could be the best way of achieving improved capacity, data rates and bit error probability. Nevertheless, very high PPM order also comes with requirements of high computing processing resource and also strict slot synchronization and error correction to ensure reliable data transmission and recovery.

ACKNOWLEDGEMENTS

The author would like to thank Jon Hamkins, B. Moision, Michael K. Cheng and Robert Daddato for their friendly assistance by answering some questions in email correspondence at the initial stage of the writing of this paper which started as a team project under the supervision of Prof. Dr. Shun-Ping Chen.

REFERENCES

1. H. Hemmati, “Deep Space Optical Communications”, Deep Space Communications and Navigation Systems, Center of Excellence, Jet Propulsion Laboratory, California Institute of Technology, Publisher: Wiley 2006.
2. A. Biswas, K. E. Wilson, S. Piazzolla, J. Wu, W. H. Farr, "Deep Space Optical Communications Link Availability and Data Volume", Deep Space Communications and

Navigation Systems, Center of Excellence, Jet Propulsion Laboratory, California Institute of Technology, The International Society for Optical Engineering, pp. 1-10, June 2004.
3. A. Biswas, and S. Piazzolla, "Deep-Space Optical Communications Downlink Budget from Mars: System Parameters", The Interplanetary Network Progress Report, pp. 1-38, June 2003.
4. R. Gallager, "Information Theory and Reliable Communication", New York: Wiley, 1968.
5. J. Hamkins, "Accurate Computation of the Performance of M-ary Orthogonal Signaling on a Discrete Memoryless Channel", IEEE Transactions on Communications, 2003.
6. C. W. Helstrom, Quantum Detection and Estimation Theory, Mathematics in Science and Engineering, vol. 123, New York: Academic Press, 1976.
7. C. C. Chen, Figure of Merit for Direct Detection Optical Channels, *The Telecommunications and Data Acquisition Progress Report 42-109, January March 1992*, Jet Propulsion Laboratory, Pasadena, California, pp. 136 151, May 15, 1992.
8. J. Hamkins, The Capacity of Avalanche Photodiode Detected PulsePosition Modulation, *The Telecommunications and Mission Operations Progress Report 42-138, April June 1999*, Jet Propulsion Laboratory, Pasadena, California, pp. 1 19, August 15, 1999.

Figures

Figure 1

Block diagram of a DSOC model

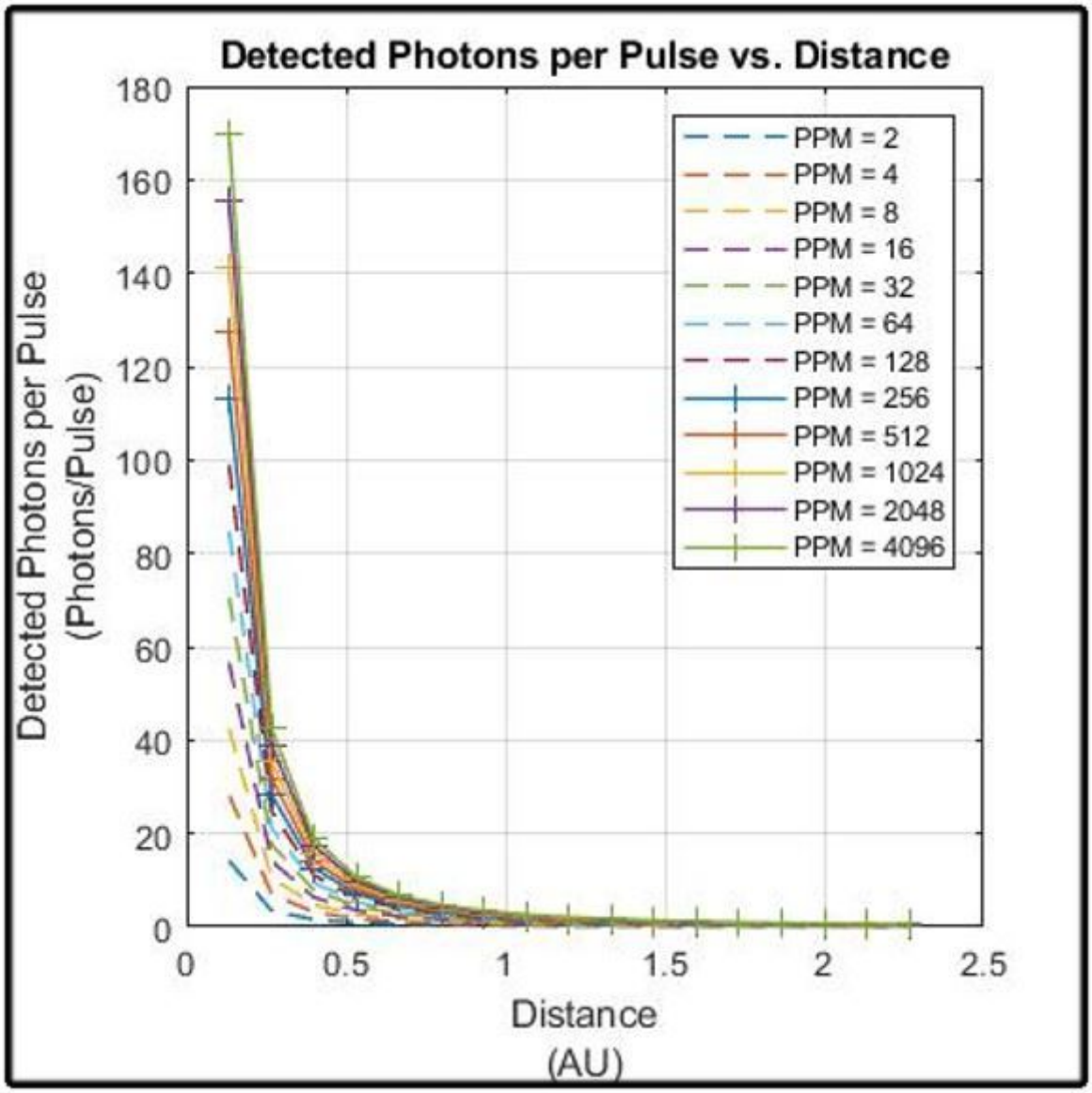

Figure 2

Photons per Pulse vs. Distance

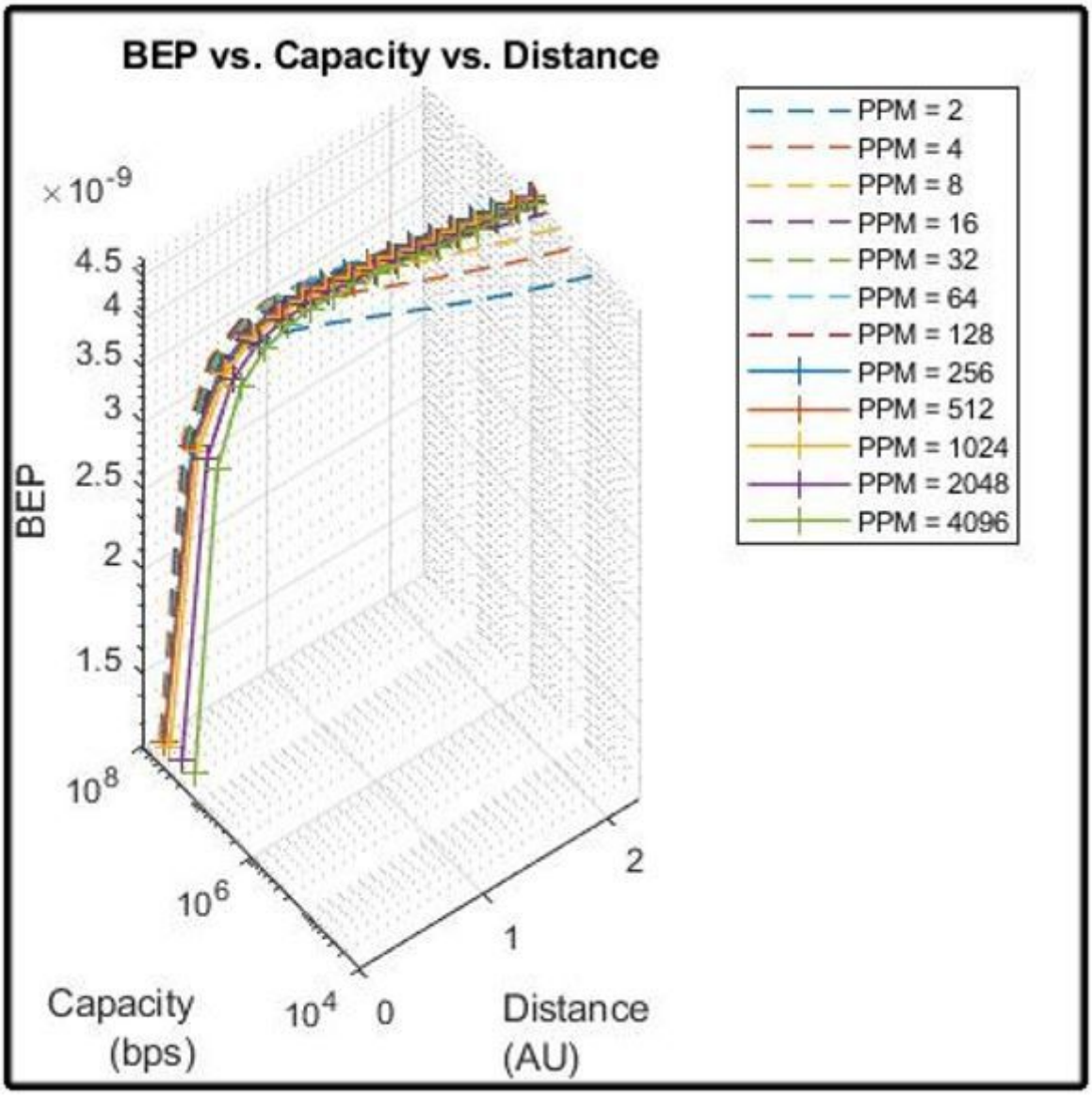

Figure 3

BEP vs. Channel Capacity vs. Distance

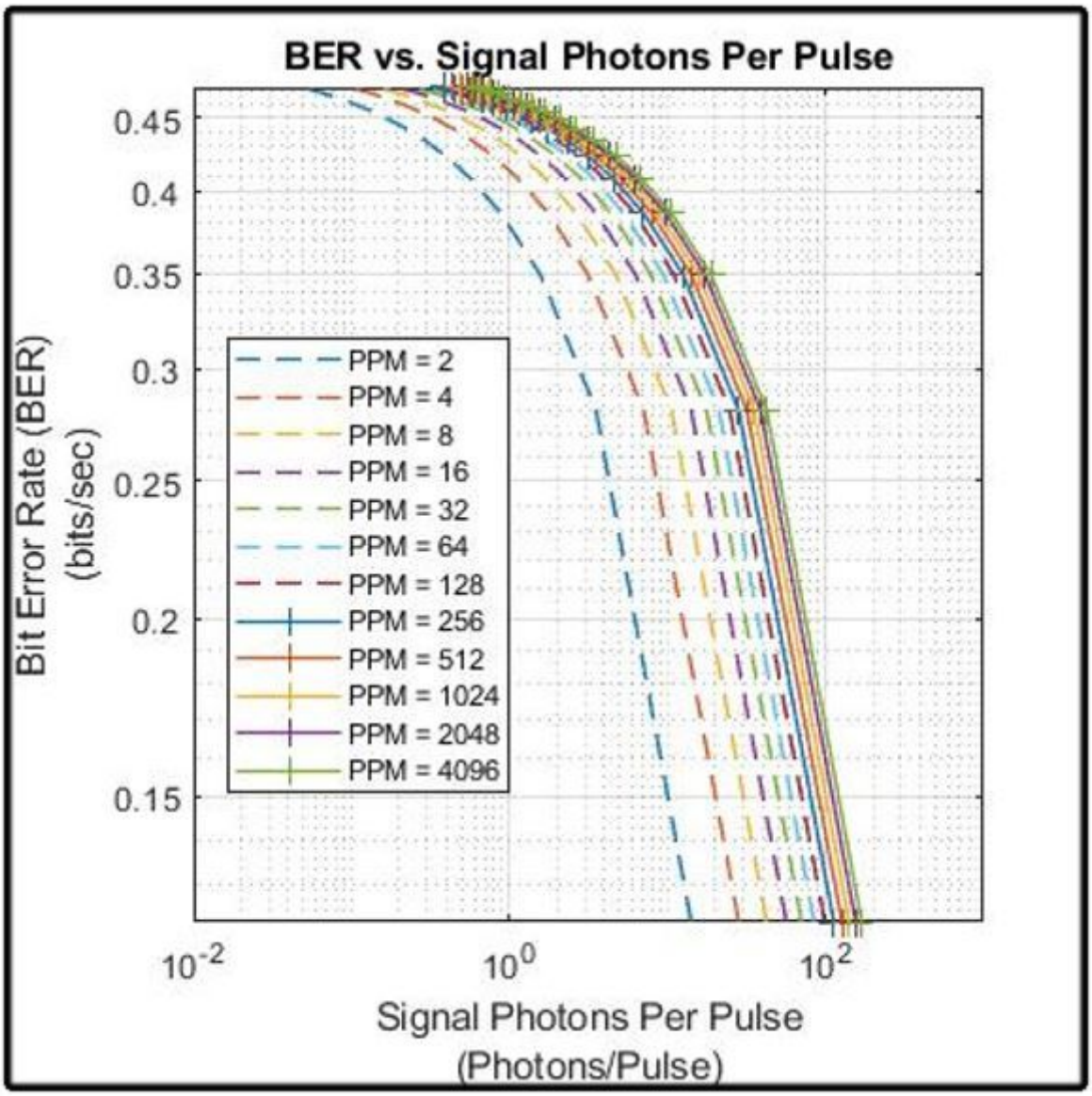

Figure 4

BER vs. Signal Photons per Pulse (Ks)

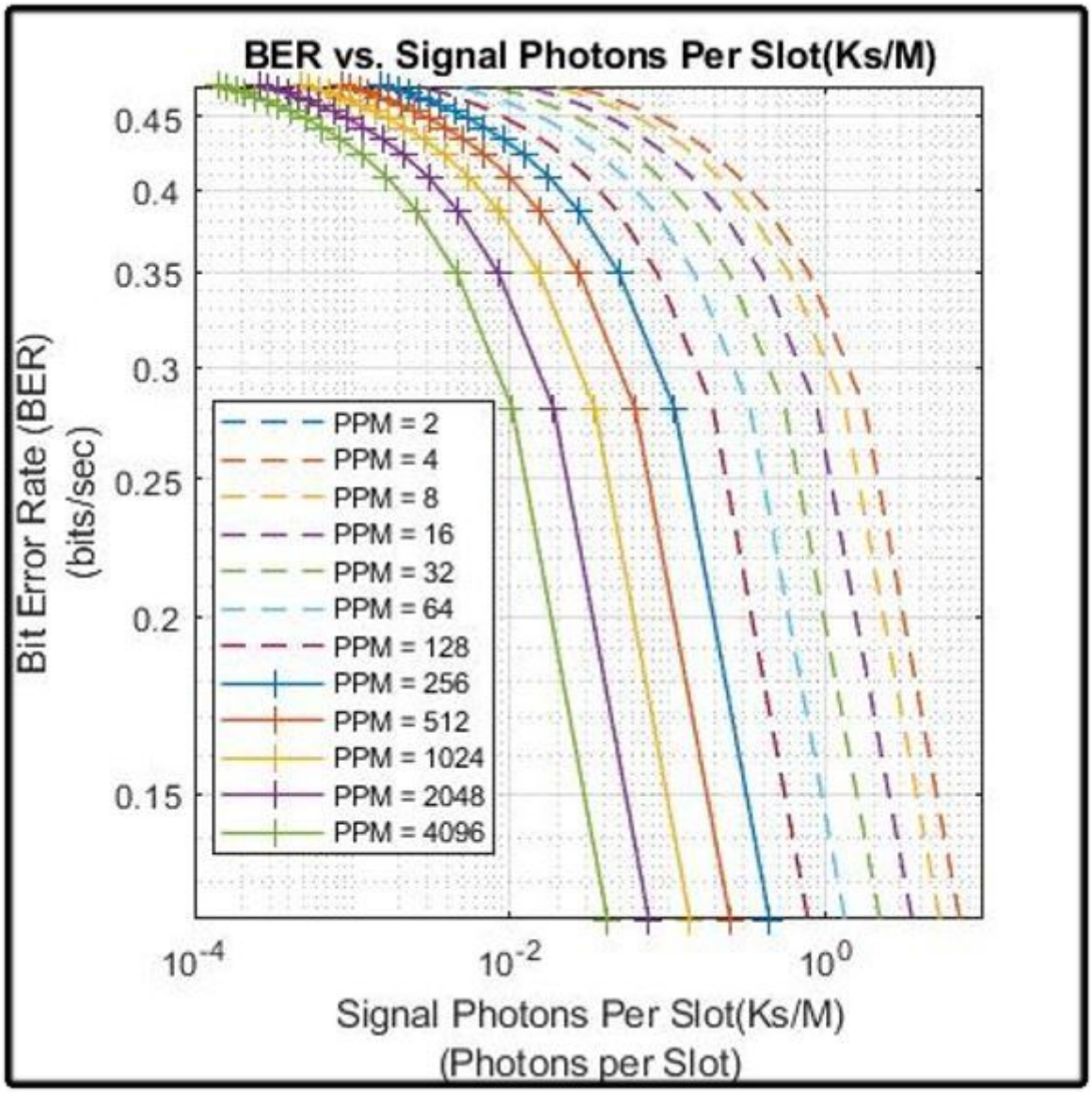

Figure 5

BER vs. Photons per Slot (Ks/M)

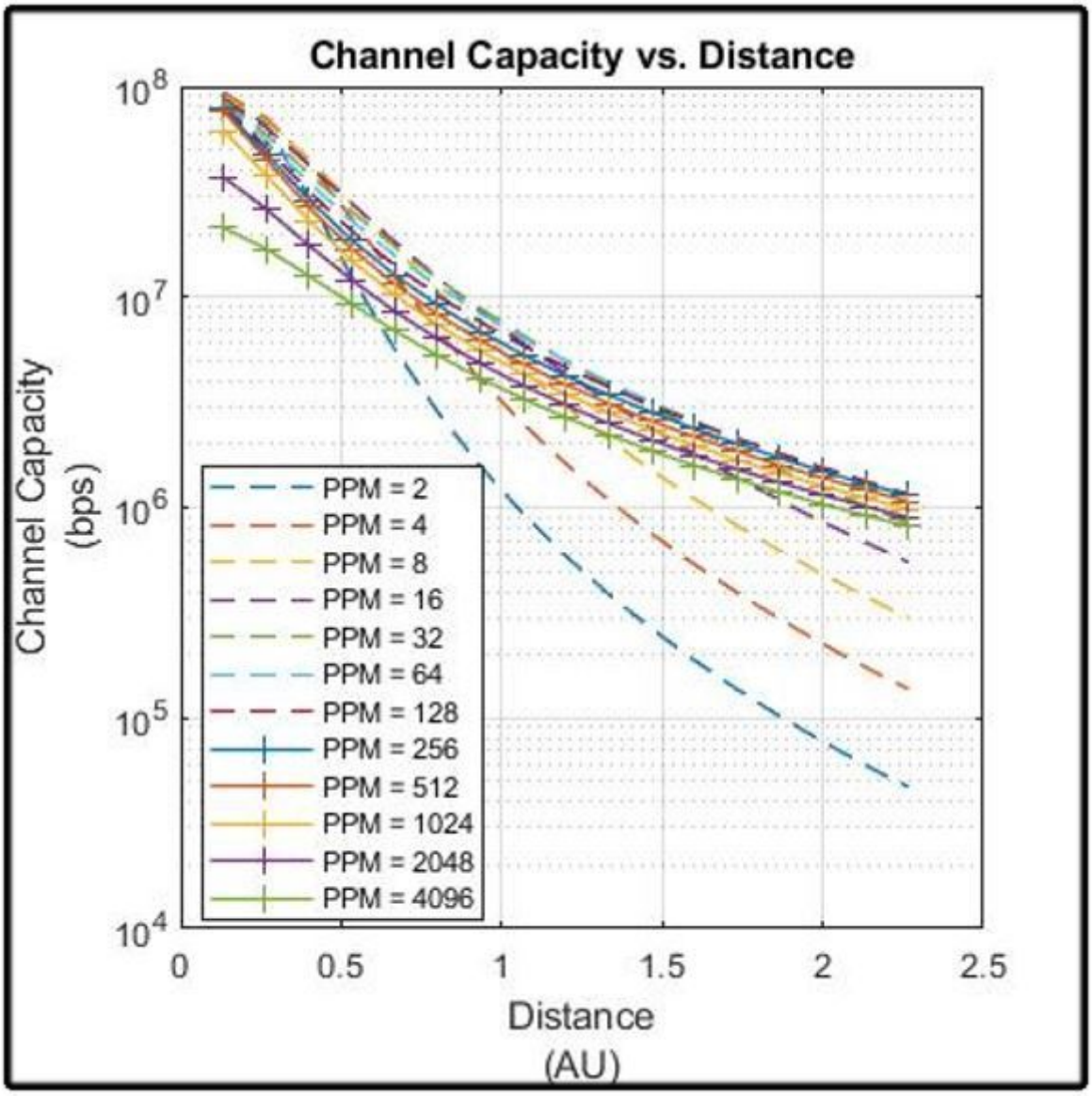

Figure 6

Channel Capacity vs. Distance

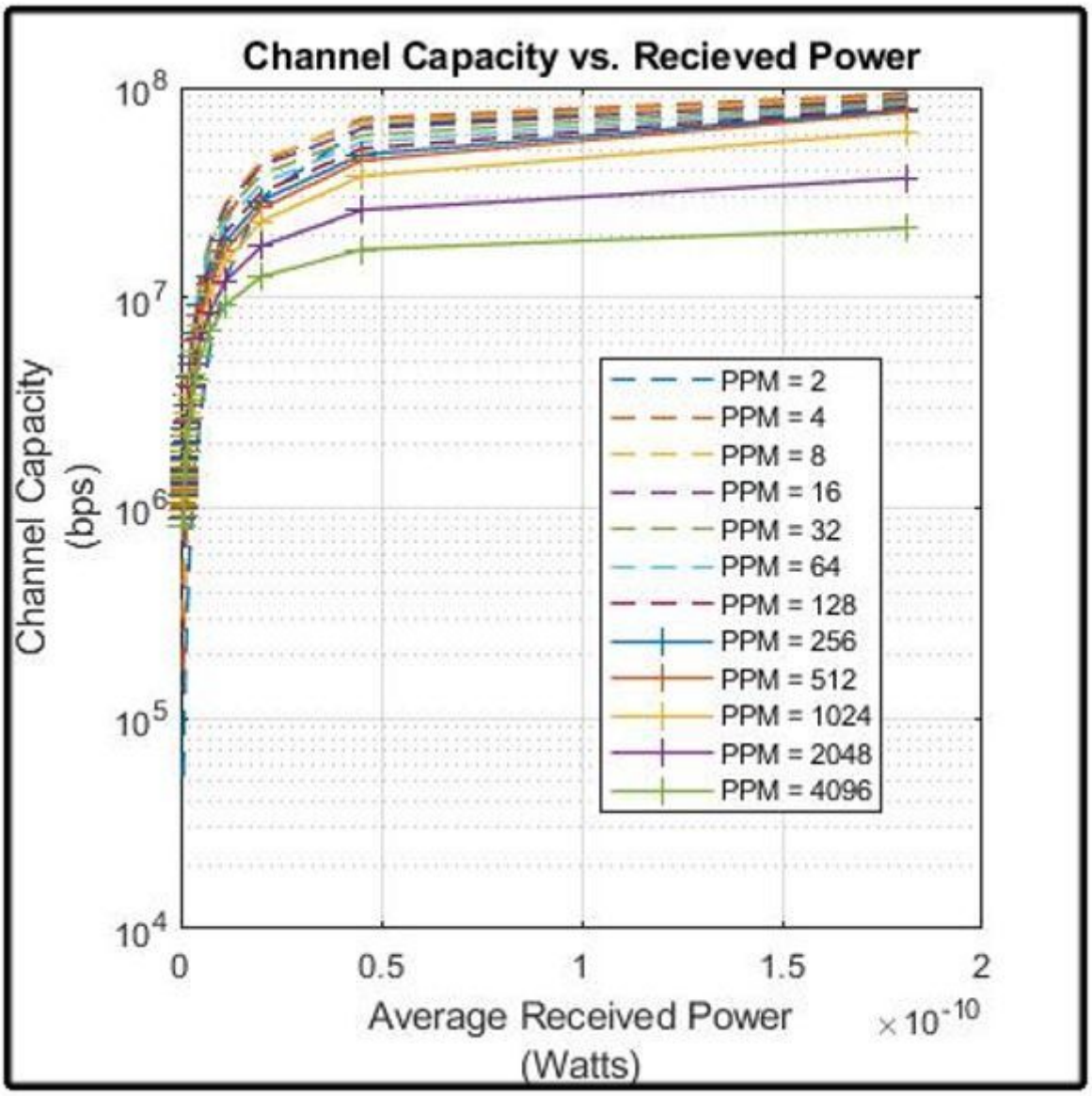

Figure 7

Channel Capacity vs. Received Power (Watt)

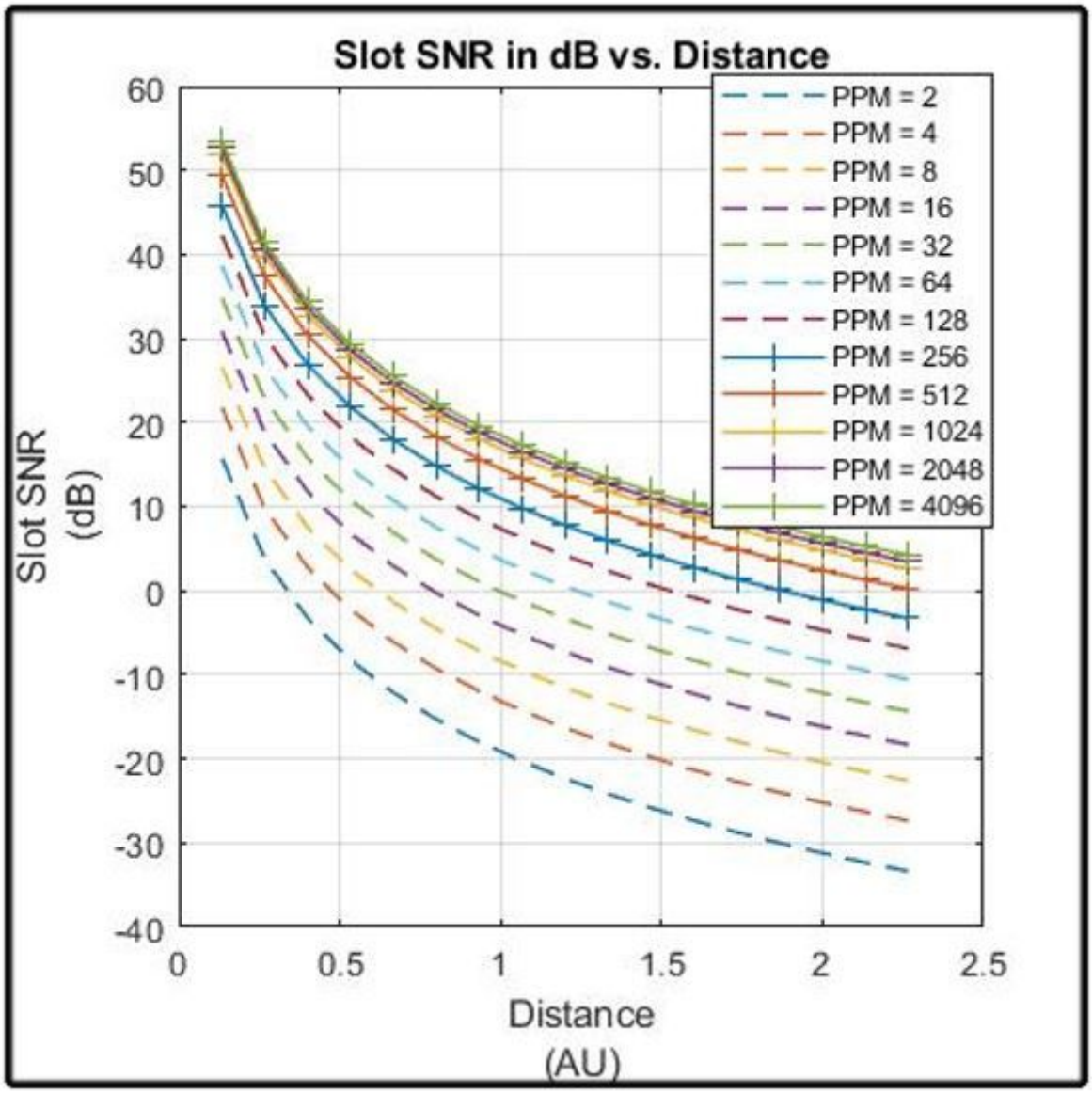

Figure 8

Slot SNR (in dB) vs. Distance

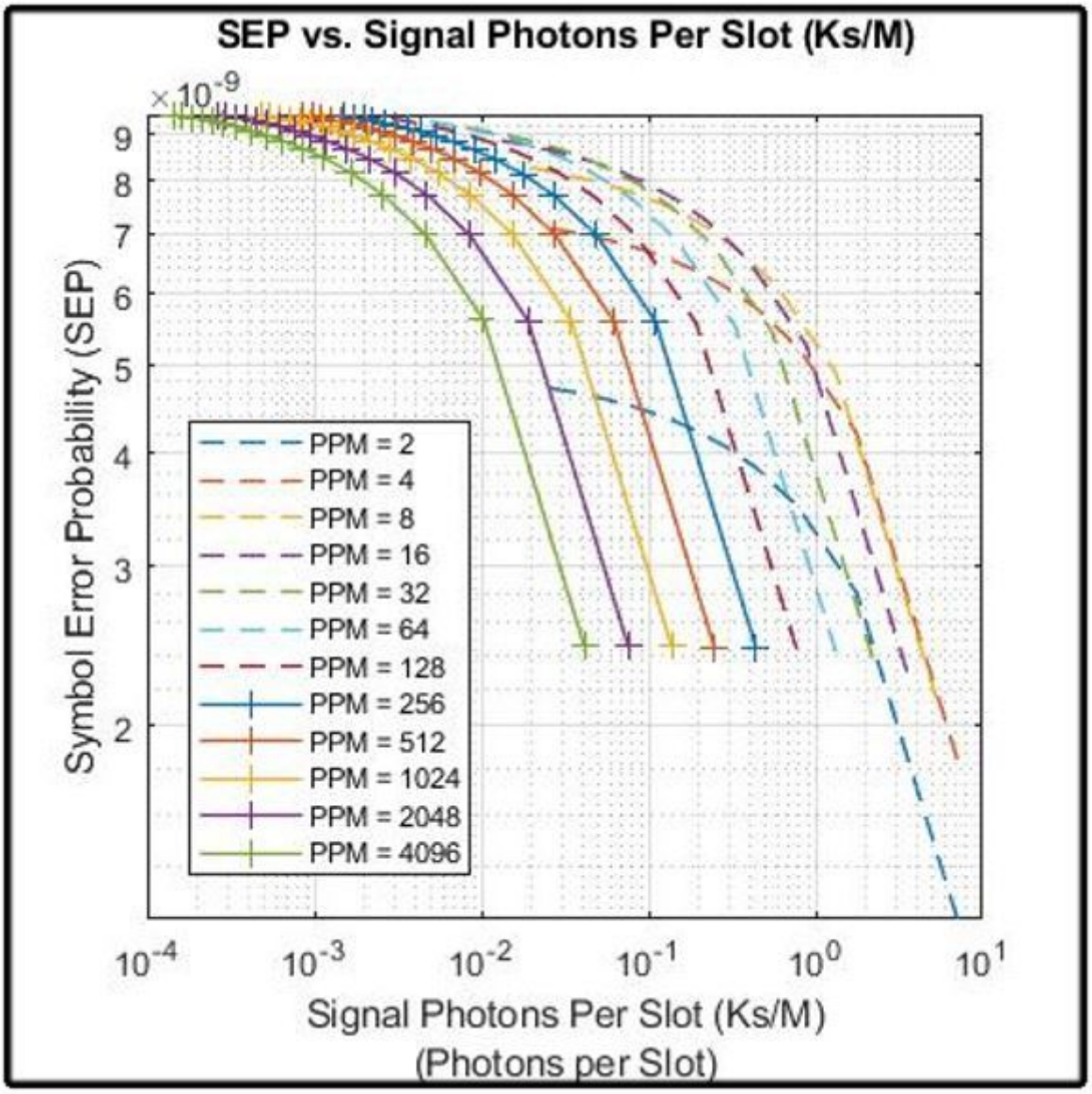

Figure 9

Symbol Error Probability (SEP) vs. Signal Photons per Pulse

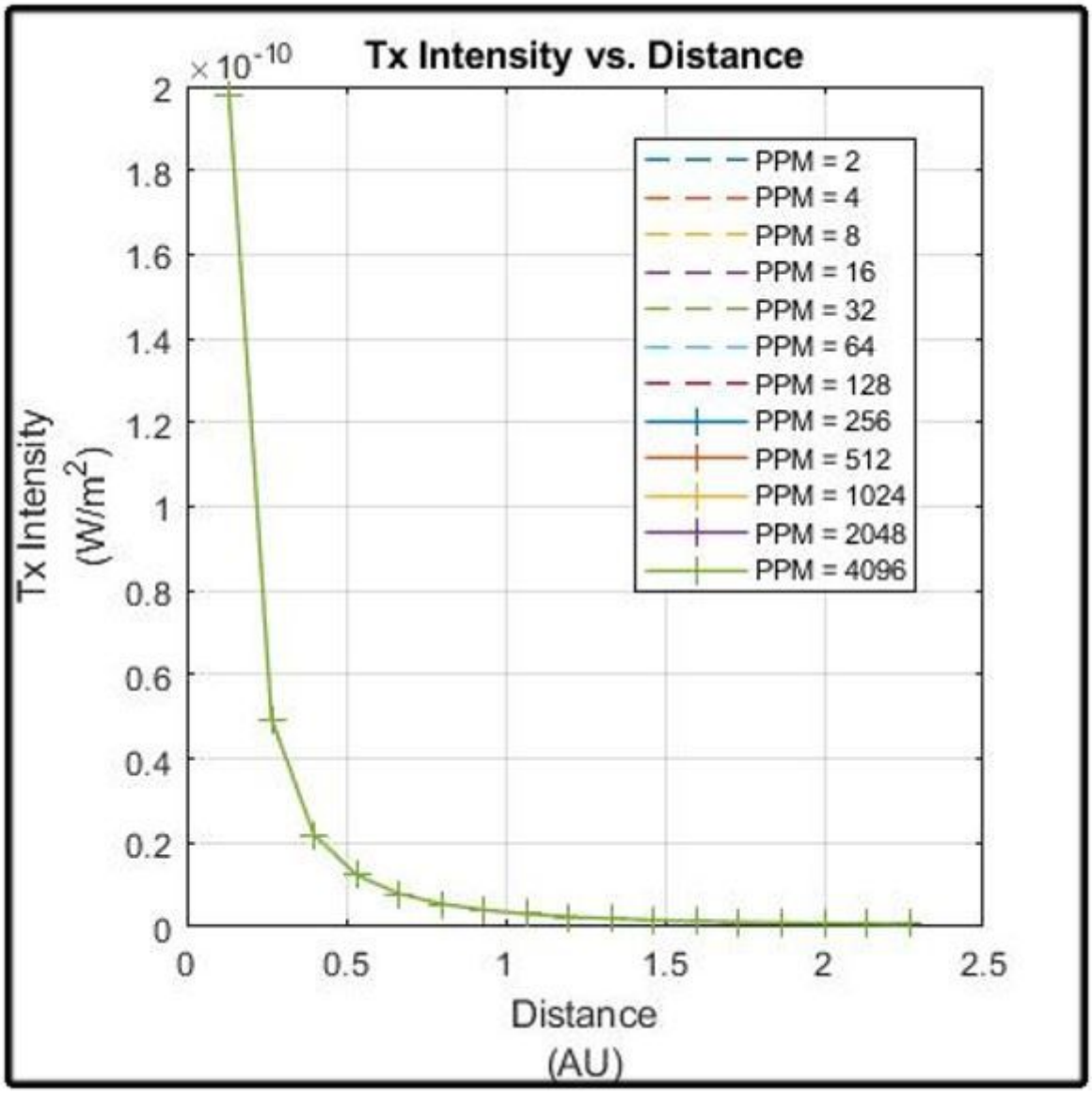

Figure 10

Tx Intensity vs. Distance

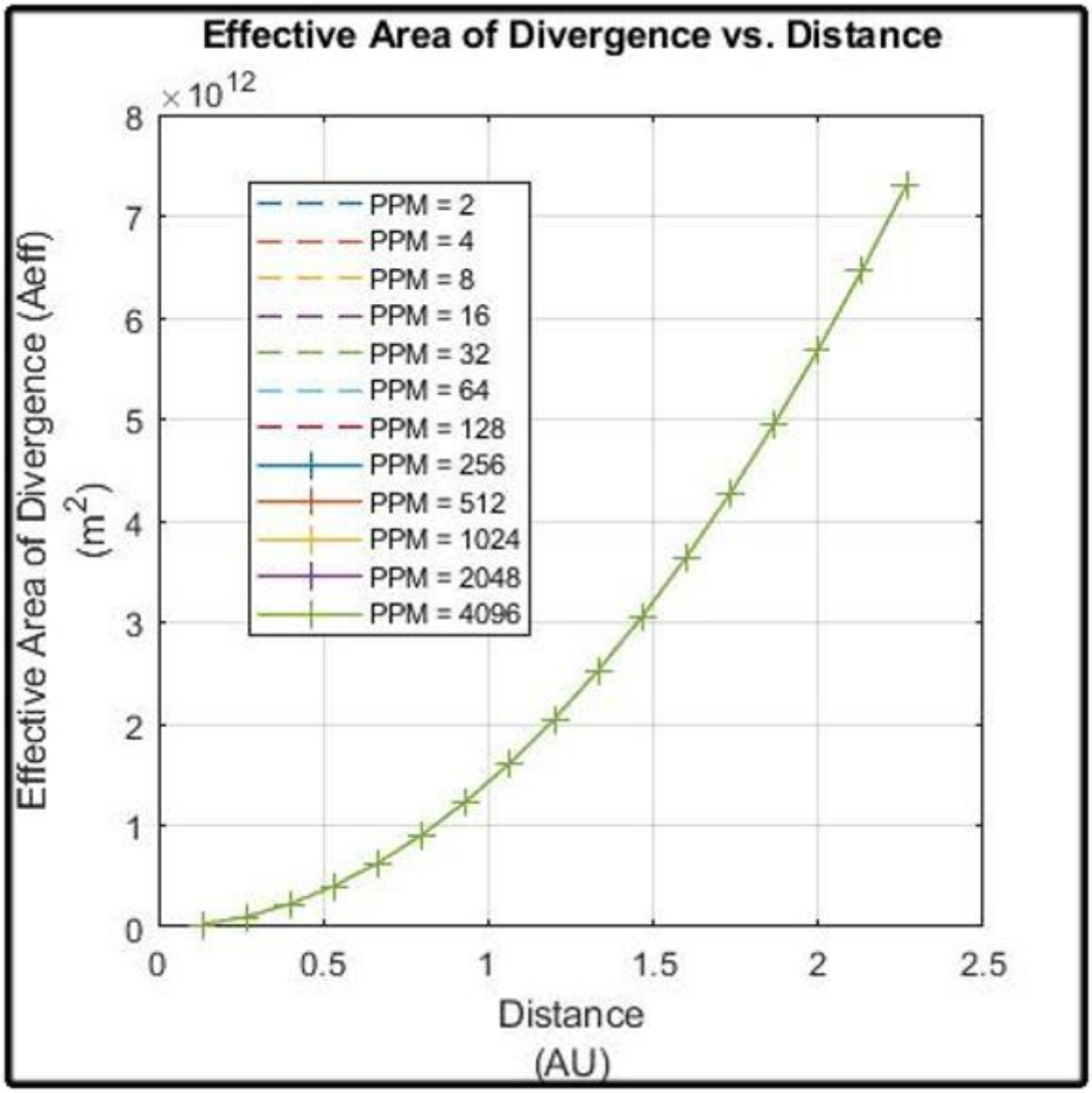

Figure 11

Effective Area of Divergence vs. Distance

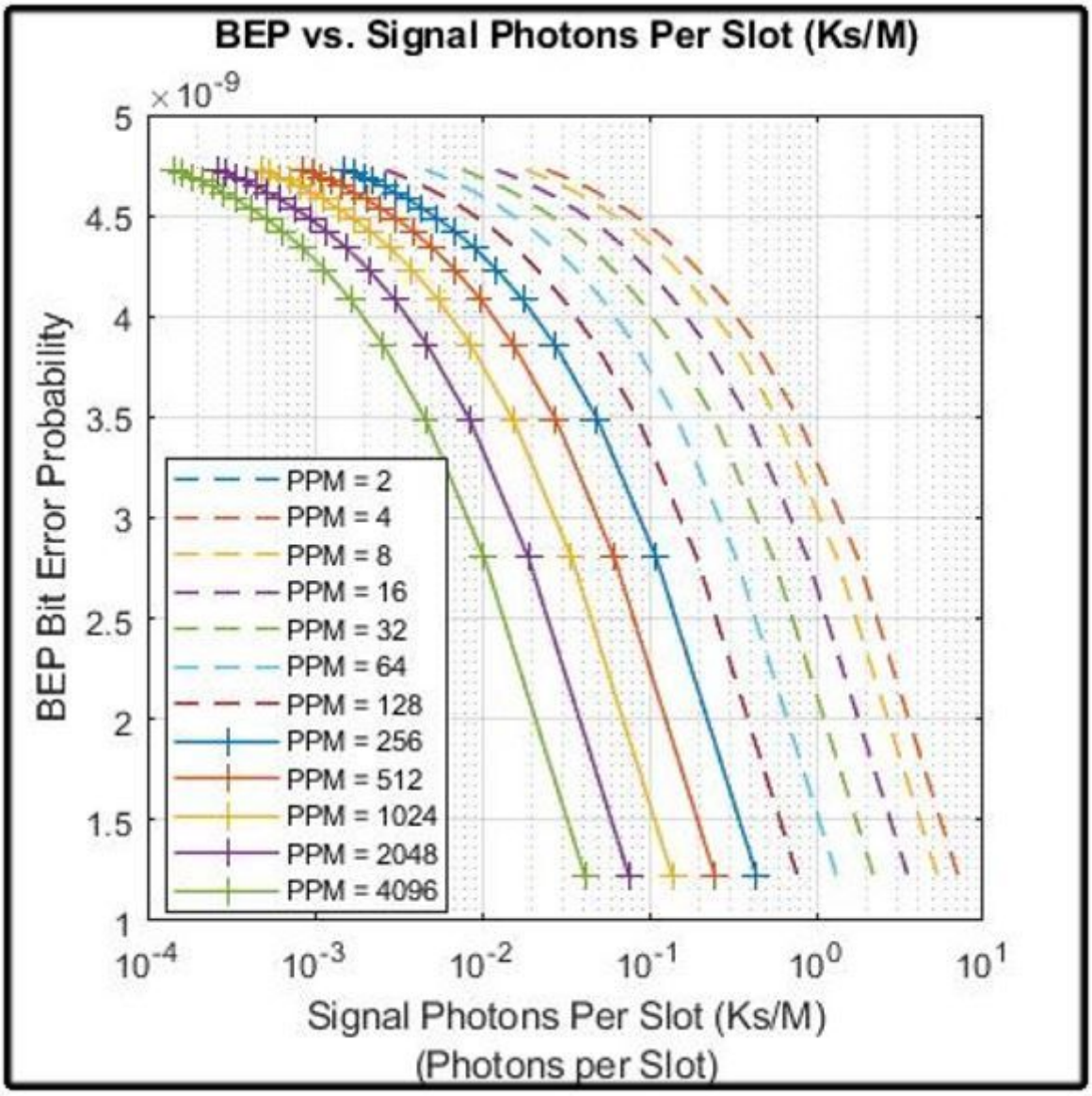

Figure 12

Bit Error Probability (BEP) vs. Signal Photons per Slot

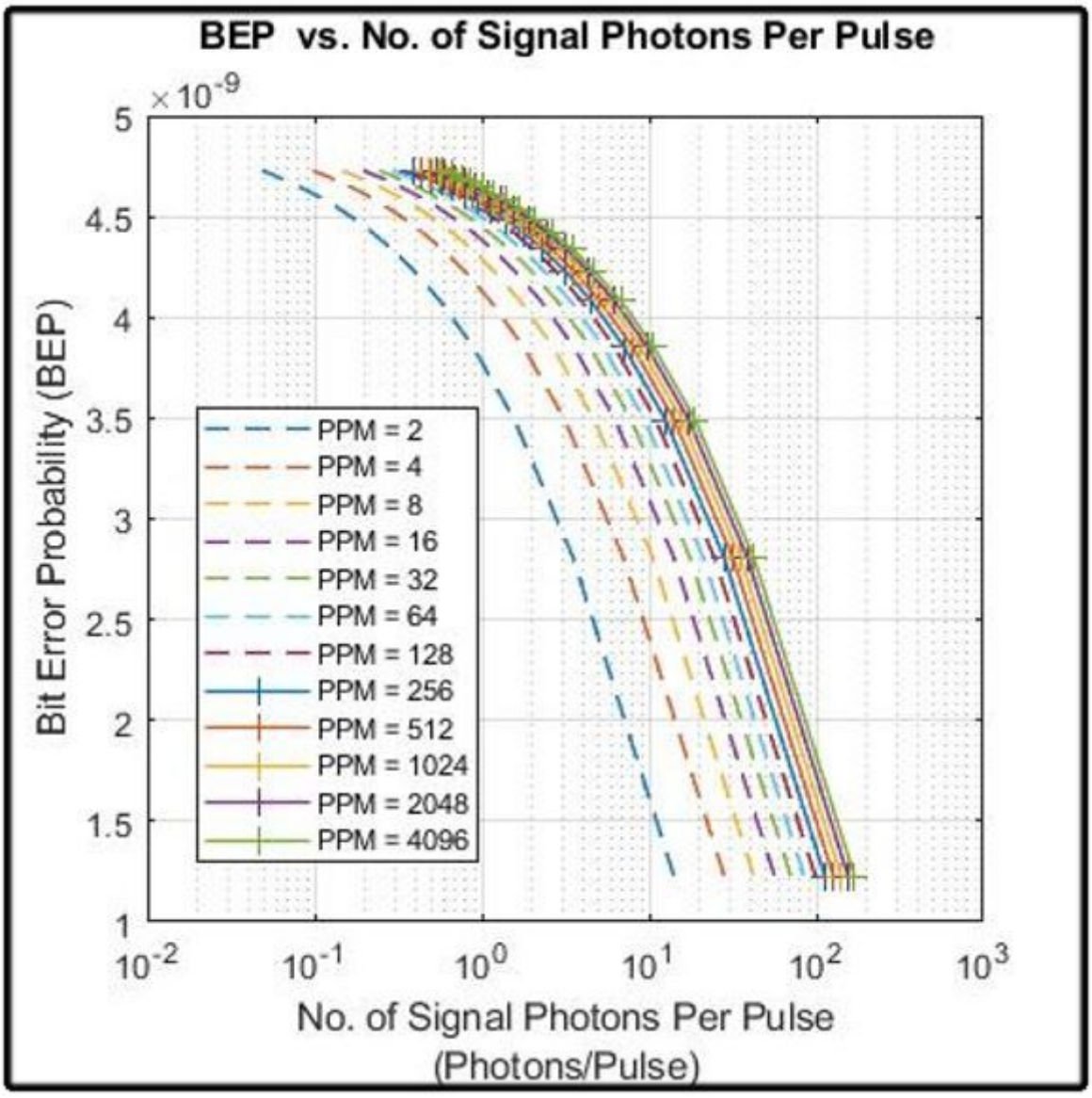

Figure 13

Bit Error Probability (BEP) vs. Signal Photons per Pulse

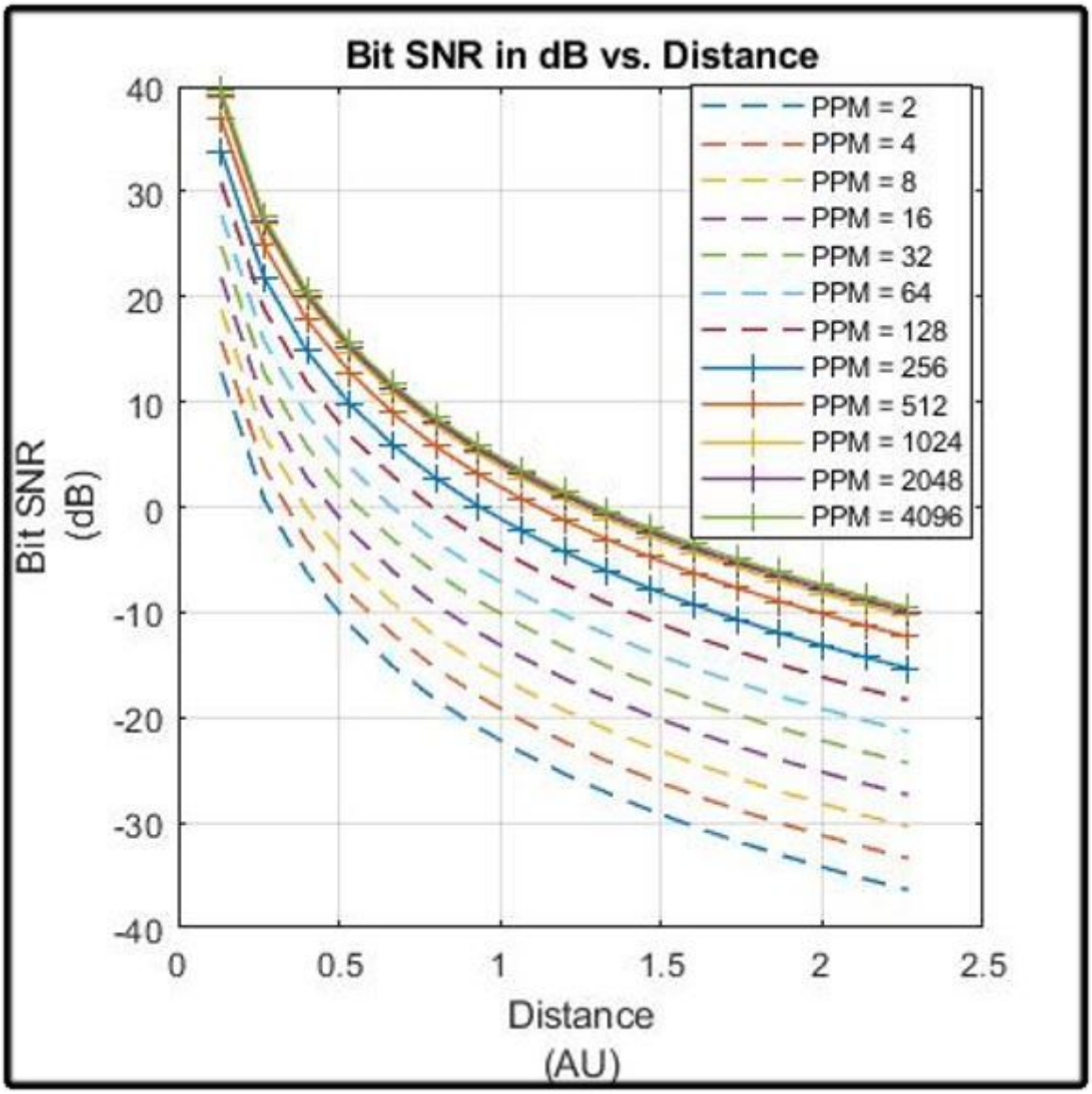

Figure 14

Bit SNR (in dB) vs. Distance

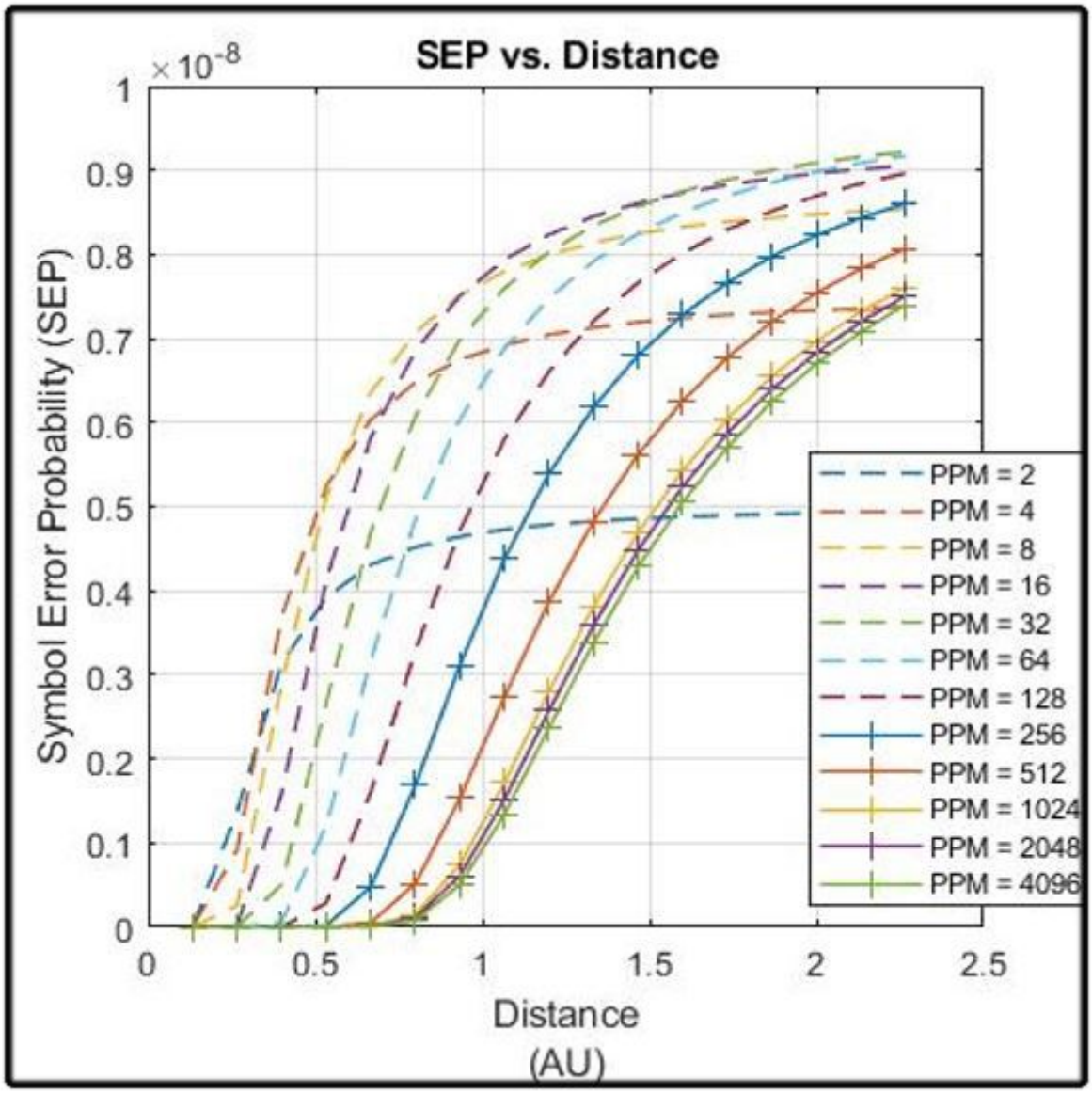

Figure 15

Symbol Error Probability (SEP) vs. Distance

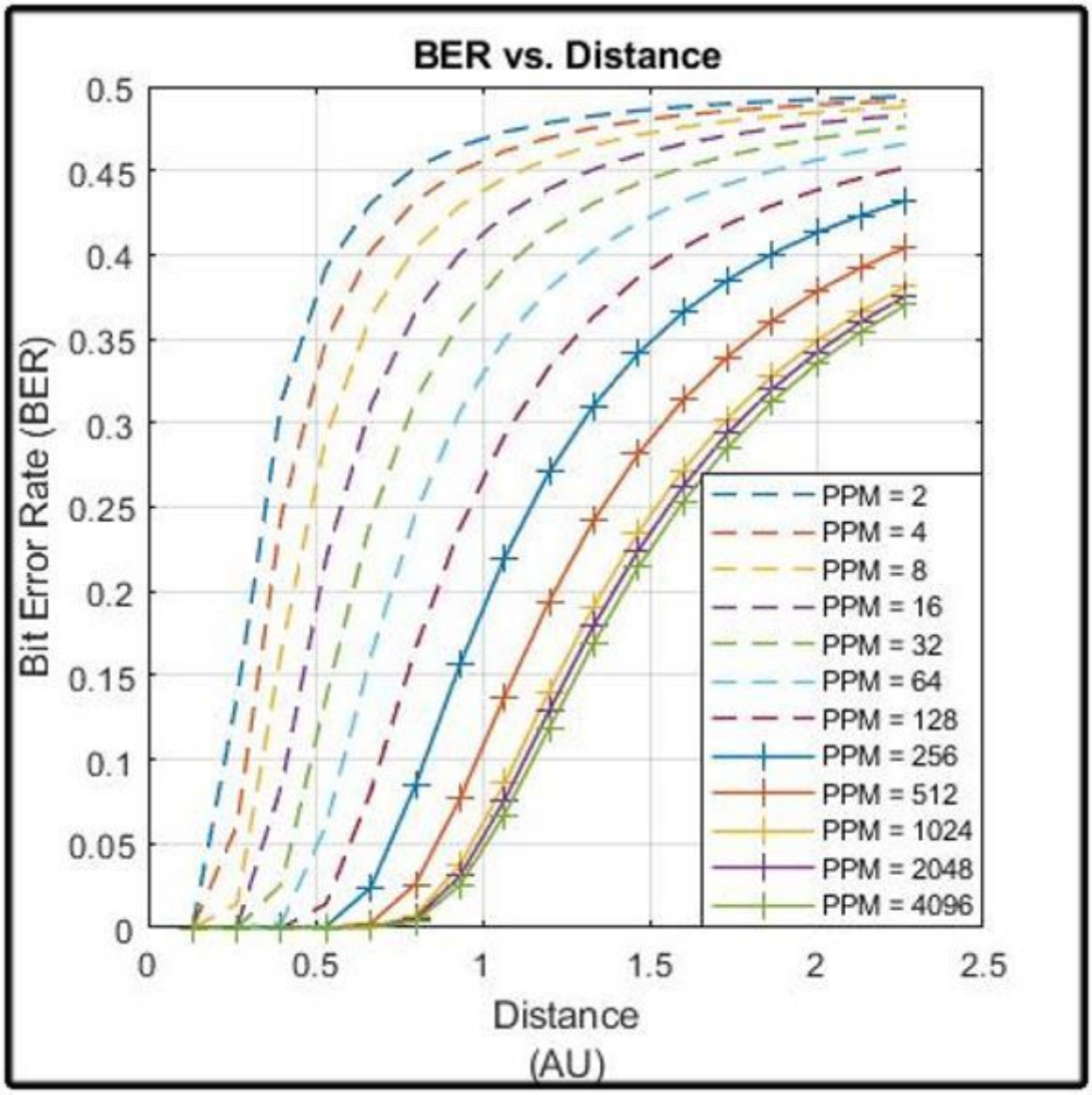

Figure 16

Bit Error Rate (BER) vs. Distance

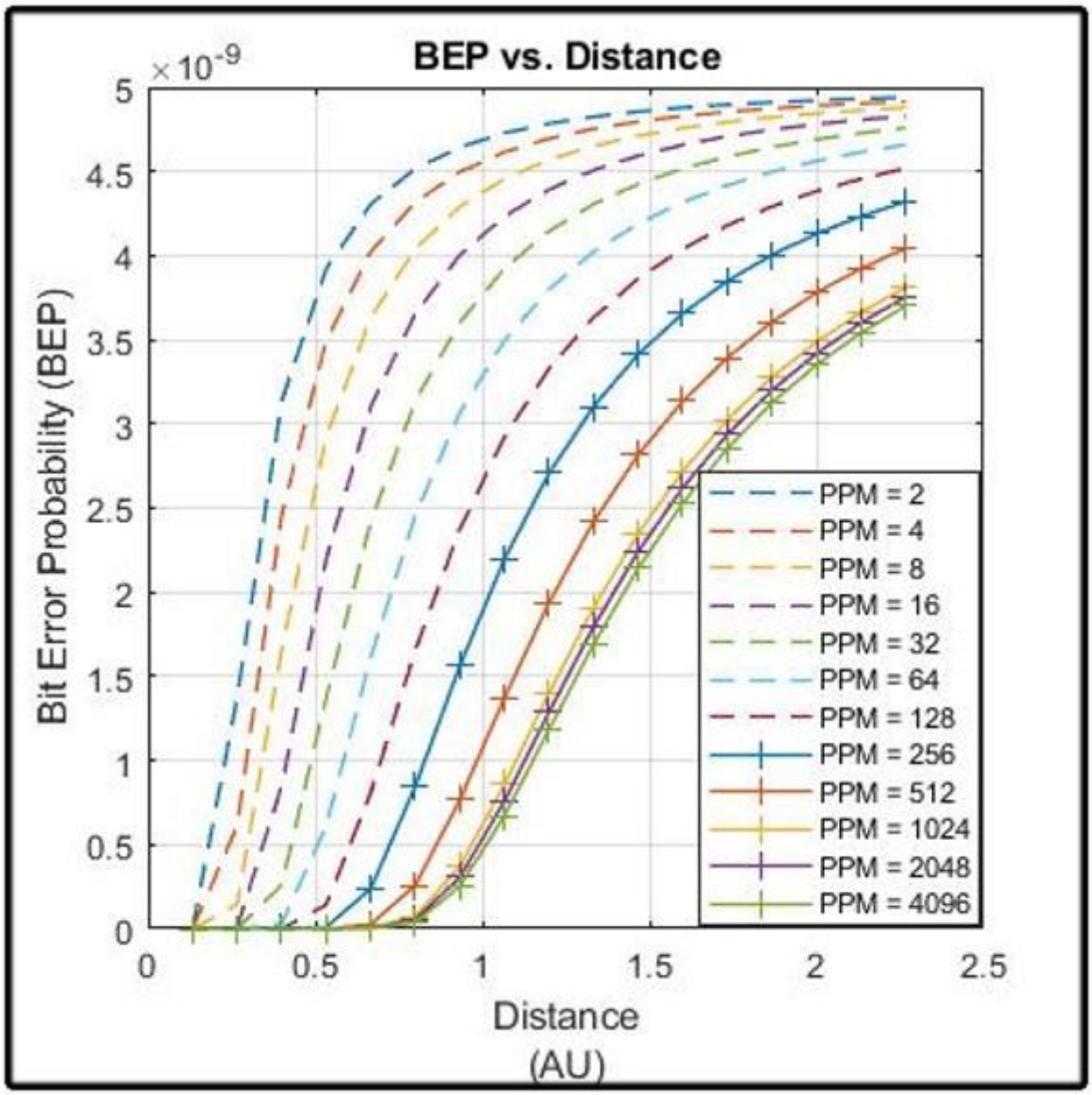

Figure 17

Bit Error Probability (BEP) vs. Distance